NASA-CR-198008

SwRI Project No. 15-5653
February 28, 1995

INTERIM
IN-91-CR
O CIT
45515
p 48

Semi-Annual Report for

DISTRIBUTION AND NATURE OF UV ABSORBERS ON TRITON'S SURFACE
Contract No. NAGW-3402

Submitted to:

NASA Headquarters
Washington, DC

(NASA-CR-198008) DISTRIBUTION AND NATURE OF UV ABSORBERS ON TRITION'S SURFACE Semiannual Report (Southwest Research Inst.) 48 p
N95-26116
Unclas
G3/91 0045515

Submitted by:

S. Alan Stern
Southwest Research Institute
Division 15 Boulder Extension Office
Geophysical, Astrophysical, and Planetary Sciences Section
1050 Walnut, Suite 429
Boulder, Colorado 80302
303/546-9670 FAX 303/546-9687

SOUTHWEST RESEARCH INSTITUTE
Instrumentation and Space Research Division
6220 Culebra Road, San Antonio, Texas 78238
(210) 684-5111 • FAX (210)647-4325

Introduction

Substantial evidence suggests that a UV Spectrally Absorbing Material (UV-SAM) exists on Triton's surface (e.g, Stern 1993; Croft, et al. 1994). This evidence is found in the positive slope in Triton's spectrum from the UV to the near-IR, and the increasing contrast in Triton's light curve in the blue and UV. Although it is now widely-thought that UV-SAMs exist on Triton, little is known about their distribution and spectral properties.

The goal of this NDAP Project is to determine the spatial distribution and geological context of the UV-SAM material. We hope to determine if UV-SAMs on Triton are correlated with geologic wind streaks, craters, calderas, geomorphic/topographic units, regions containing (or lacking) volatile frosts, or some other process (e.g., magnetospheric interactions). Once the location and distribution of UV-SAMs has been determined, further constraints on their composition can be made by analyzing the spectrographic data set.

To accomplish these goals, various data sets will be used, including Voyager 2 UV and visible images of Triton's surface, IUE and HST spectra of Triton, and a geologic map of the surface based on Voyager 2 and spectrophotometric data. The results of this research will be published in the planetary science literature.

Research Progress

We began this project by performing a global survey of Triton's surface to look for large scale UV-SAMs regions. The primary data set used for this task consisted of Voyager 2 ISS mosaic images of Triton's surface made using the UV (3500 Å) and CLEAR (5600 Å) filters (Figure 1). These mosaics cover mainly the equatorial region of the satellite.

The UV-SAM on Triton has a relatively low UV and high visible albedo. Therefore, the locations of preferentially-high UV-SAM concentrations should correspond to regions where the UV-filter brightness is anti-correlated with visible brightness in the Voyager mosaics.

Two methods were used to accomplish this comparison. First, the UV and CLEAR mosaics were converted to contrast maps to enhance their albedo variations. This was done by subtracting an average brightness followed by normalization by the average. Potential UV-SAMs regions were further enhanced by dividing the difference of the contrast mosaics by their sum. The resulting "correlation map" shows broad regions, particularly near 0° longitude, that we conclude may represent the first identification of UV-SAM source regions on Triton.

Next, a second, more quantitative, method was used to determine if the regions detected by the method described above are real indications of UV-SAMs. To do this we looked for a correspondence between (i) regions in the UV mosaic that are between 1 and 2 standard deviations (σ) darker than the average albedo and (ii) regions in the CLEAR mosaic that are 1-2 σ brighter than average (cf. Figures 7-9 of Appendix 1). The results of this analysis show that the possible UV-absorbing region around 0° longitude also passes this test, confirming the findings of the first method described above.

It was recognized that the global comparisons described above could miss small-spatial-scale UV-SAM regions. Therefore, small sub-regions ranging in size from $\simeq$500×500 km to $\simeq$2000×2000 km (at the equator) were tested for anti-correlated albedo behavior. Using a sub-region size of $\simeq$2000×2000 km revealed a distinct UV-SAM region $\simeq$700×1900 km in size centered near +20° longitude and −25° latitude (Figure 2). Significantly, this region is colocated with a distinct geological unit on Triton containing maculae (spotted terrain) and wind streaks, as identified in a geologic map provided by CoI Schenk. Furthermore, the UV-SAM region abuts a highly reflective region possibly containing clean ices, suggesting a possible volatile transport relationship. We presented these results at a recent scientific meeting (Flynn et al., 1995; see Appendix 2) and they are currently being written up for the proceedings of

the conference.

Future Work

The remaining steps in our analysis are: (1) To analyze high-resolution images of Triton's surface corresponding to the UV-SAM region we have identified in order to determine whether smaller scale features, such as maculae or wind streaks, are responsible for the UV absorption; (2) to correlate the locations of the UV-SAM source region with the spectroscopic data set to place further compositional constraints on the UV-SAM material; and (3) to develop a volatile transport scenario to explain the apparently related distribution of UV-SAM material and neighboring clean ices.

Following this, CoIs Buratti and Schenk will join us in Boulder to complete the comparison of UV-SAM locations to geologic and seasonal volatile transport boundaries. Our results will then be written up and published in a refereed scientific journal.

References

Croft, S.K., et al., 1994. "The Geology of Triton." In *Triton* (U. Az. Press, ed. D. Cruikshank), in press.

Flynn, B., A. Stern, B. Buratti, P. Schenk, and L. Trafton, 1995. The Spatial Distribution of UV-Absorbing Regions on Triton. International Conference on Solar System Ices, Toulouse, March, 1995.

Stern, S.A., 1993. Properties and Tentative Identification of the Strongly UV-Absorbing Surface Constituent on Triton. *Icarus*, **102**, 170-173.

Figure Captions

Figure 1. Mosaic constructed from 10 Voyager 2 ISS images taken through the UV (3500 Å) filter. The images were taken in August 1989 prior to closest approach to Triton.

Figure 2. Correlation map constructed using $\simeq$2000$\times$2000 km sub-regions, revealing a distinct UV-SAM region $\simeq$700$\simeq$1900 km in size and centered near $+20°$ longitude and $-25°$ latitude.

Clear 5%>Average, UV 5%<Average

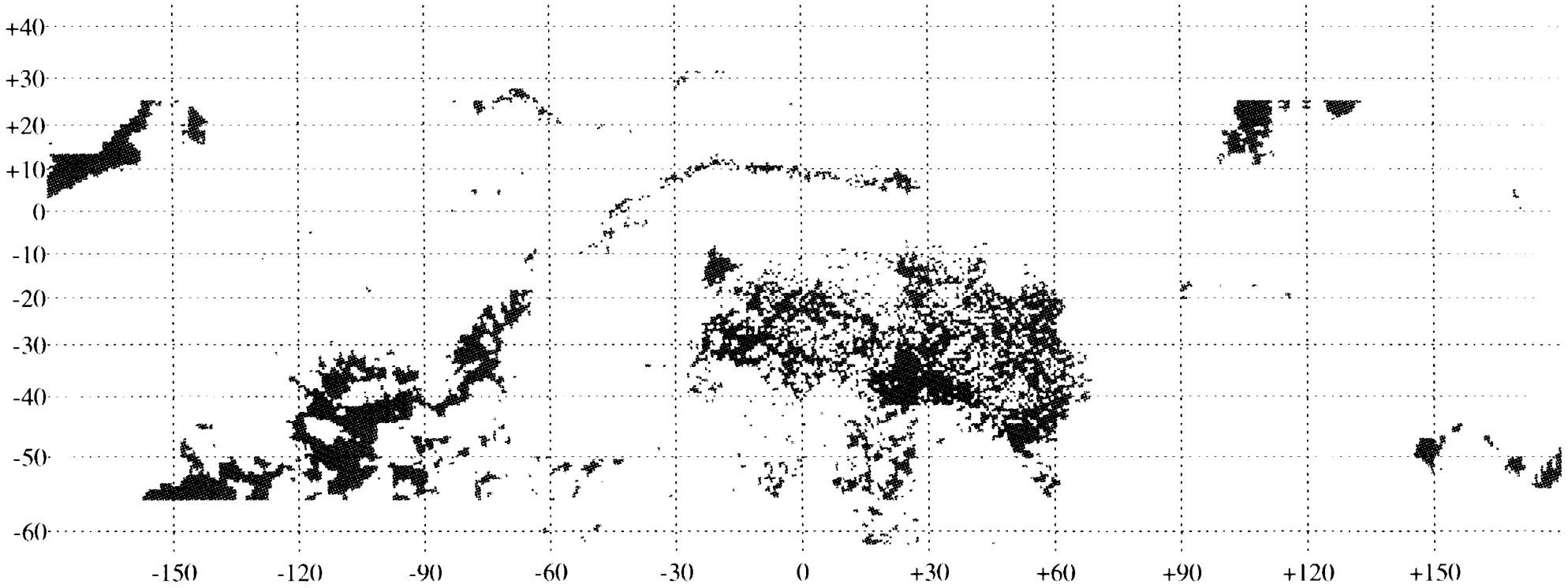

Fig.2

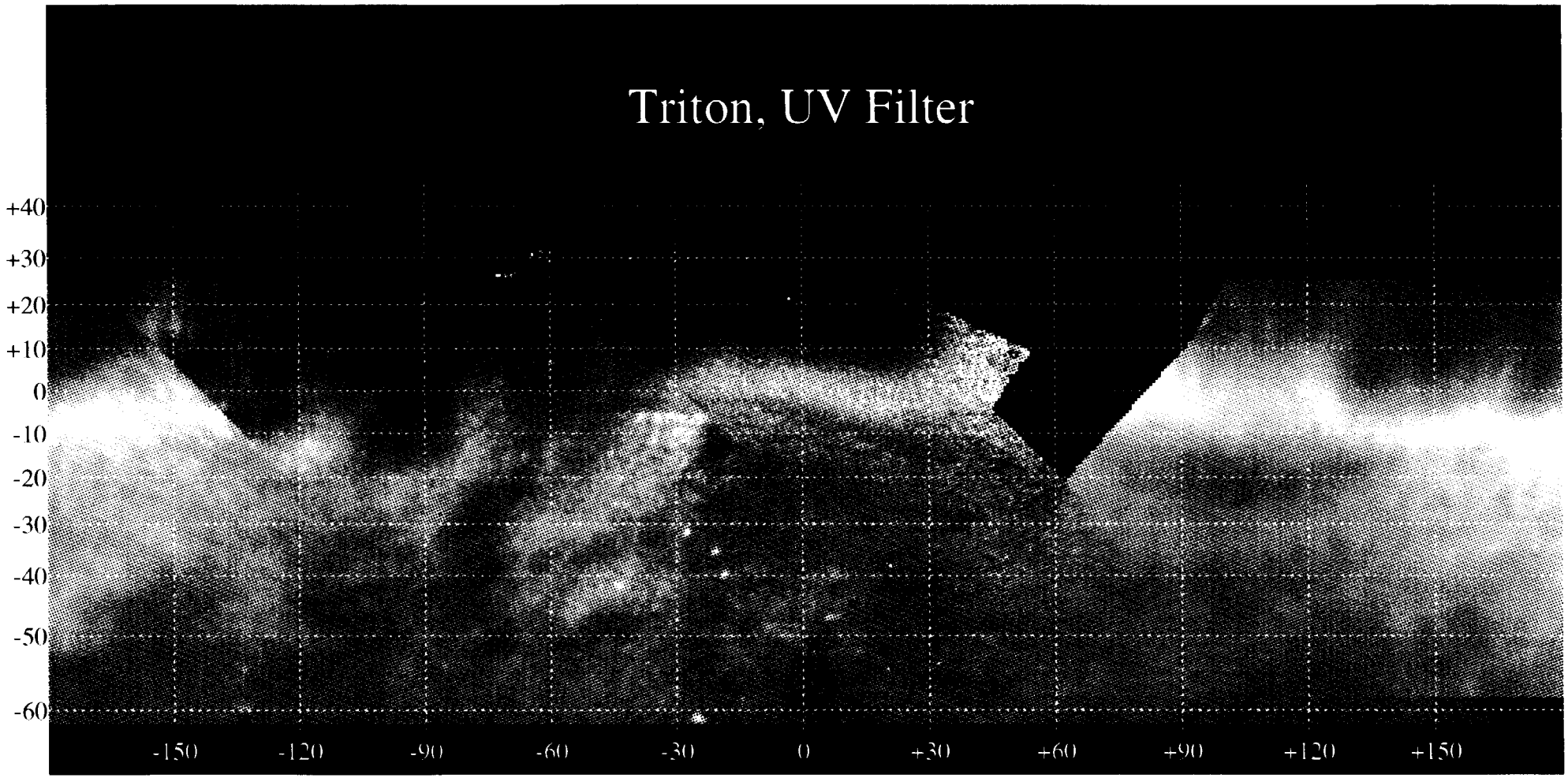
Triton, UV Filter
+40
+30
+20
+10
0
-10
-20
-30
-40
-50
-60
-150
-120
-90
-60
-30
0
+30
+60
+90
+120
+150

Fig.1

Appendix 1

Preliminary results of search for large scale UV absorbing regions on Triton

Spatial Resolution of UV Absorbers on Triton

Clark Snowdall
May 2, 1994

Table of Contents

Abstract 1

Introduction 2

Data and Procedures 4

Results and Further Work 11

References 14

Captions to Figures 15

Figures 16

Abstract

Neptune's moon Triton is very unlike any other body studied in the solar system. It is hoped that it might yield support to theories on the evolution of the solar system. One of its most interesting features is the existence of ultraviolet (UV) absorbing materials on its surface. We attempted to create a map of these UV absorbing areas using Voyager II data. We wanted to compare their location to geological maps as well as place constraints on what these materials might be. Our analysis resulted in finding no clear spatial distribution of UV absorbing material on Triton.

I. Introduction

In recent years a number of ideas involving the origin and ongoing evolution of the solar system have been developed and explored observationally. One of the most important is the Kuiper Disk theory (Yeomans, 1991). This theory suggests that beyond the Neptune there is a belt of icy planetessimals, solar orbiting bodies between a few and a few hundred kilometers in diameter. This band of planetessimals has been the suggested source of several solar orbiting comets.

It is suggested that Triton, a moon of Neptune, could be one of these icy planetessimals that was captured by Neptune's gravity. Triton's icy composition is not consistent with Neptune's composition. This suggests that it was not formed when Neptune was formed. Triton also has a highly elliptical orbit around its host, indicating capture rather than co-formation as its source.

Triton could also be used to give insight into the Pluto/Charon system. Both Triton and the Pluto/Charon system display the "dirty snowball" composition that is indicative of comets, yet so unlike the neighboring outer planets. Pluto's elliptical orbit again suggests capture. With these similarities some have proposed that Triton and Pluto/Charon are of the same stock, therefore studying one gives information on the other. With the Pluto Fast Fly-by still in its infancy, Voyager II's fly-by of Triton might be the best study of a Pluto-like object we will have for at least another fifteen years.

The goal then is to understand Triton, its composition and the processes at work on its surface. Voyager II's fly-by demonstrated

that Triton has a varied and active surface (Croft, Kargel, Kirk, Moore, Schenk, & Strom, 1993). One of the most intriguing aspects of this surface is the existence of ultraviolet (UV) absorbing materials. We want to know what role these substances play on Triton. Are they related to the active geysers? Are they created near craters? Are they photochemically active? The first step to finding answers to these questions is to understand where these substances are located.

This thesis examines the spatial distribution of UV absorbing material on the surface of Neptune's moon, Triton. UV absorbers are substances that strongly absorb at wavelengths less than 400nm. Our goal is to create a surface map showing areas of UV absorption. We also hope to place more constraints on what these materials might be.

We already know there are UV absorbing substances on Triton's surface. The primary evidence of this is Triton's strong red biased reflectance. This slope in its spectrum, going from high reflectance in the visual to low reflectance in the UV, can be readily seen in fig. 1. This slope seems to start after about 490nm (Stern, 1992) and drops off to near zero around 260nm, fitting our UV absorber stipulation of absorption below 400 nm.

Another piece of evidence for UV absorbers is the large amplitude of the moon's lightcurve in the UV as compared to visual wavelengths. A celestial body's lightcurve is its albedo plotted against its rotational phase. Triton's high amplitude lightcurve in the UV has been confirmed a number of times (fig. 2). Hillier points out in his paper that the UV light curve amplitude is nearly 7% while the visual hovers under 4% (Hillier, Veverka, & Helfenstein, 1991). The

UV reflectance of Triton is already quite low; widely varying reflectance further points to UV absorbers as responsible for the low points in the lightcurve.

Voyager II confirmed the existence of CH_4 and N_2 (Thompson & Sagan, 1990). C_2H_2,CO,CO_2 and H_2O are also suspected to be surface constituents. However, these substances do not absorb in the UV (fig. 3a). There are several candidates for UV absorbers (fig. 3a&b). Laboratory studies point to a variety of organics, several sulfur compounds, NaCl and some sodium nitrates, and certain refractory minerals (Stern, 1992). The most probable candidate for UV absorption at this time is SO_2 (fig. 3c).

II. Data and Procedures

The method of analysis was evident considering the spectral reflectances of some of the suspected UV absorbing materials on Triton's surface: find places that reflect strongly above 400nm and areas that absorb strongly below 400nm. We compared a high resolution visual image of Triton with its UV counterpart and searched for places where the UV image was relatively dark and the visual image was bright. These regions would exhibit UV absorption while excluding ordinary ices. The comparison with the visual image was necessary to make sure that areas on the surface that were dark in the UV were not dark across all wavelengths; something that might be caused by surface shadows or the position of the spacecraft when the image was taken.

We chose data compiled from Voyager II images taken during its flyby of Neptune in August of 1989. Our primary data set was a series of three mosaics created from Voyager II's narrow angle camera images. Each mosaic was created by carefully piecing together separate images from different angles into one image showing the moon's entire surface. The mosaics were created using images taken with different filters: one taken with Voyager II's green filter, another with the clear filter and the third with the UV filter. The transmittance curves for these filters are shown in fig. 4. These tranmittances provide a clear break at 400nm, complying with our search of UV absorbers.

The mosaics were sent via file transfer protocol over the Internet to *image1* , our primary imaging computer in the space science section at Southwest Research Institute. They came as SUN raster files that were read into our image processing software. In the three mosaics each pixel was represented by two bytes. When the data arrived the high byte was in the second place, confusing our imaging software. In order to get the data in the proper format for the imaging software, the byte pairs for each pixel had to be swapped after being read.

NASA's Jet Propulsion Laboratory (JPL) has a standard program called VICAR that was used to radiometrically correct the original Voyager II images for the effects of spacecraft's Vidicon narrow angle camera. This program corrects for the light transfer function for each pixel and makes the response linear (the Vidicon camera was exponential in its response). This step returned the raw images to what the camera actually recorded. The images were corrected

shortly after they were first downloaded from Voyager II and have since been placed on a JPL server for general access.

Some of these images were then pieced together into mosaics, showing most of the surface of Triton. The images used to create the mosaics are listed in table 2 together with their time to closest approach, image catalog number, and filter. They were cut up and laid out in Mercator projections. Because of this, areas near the poles were stretched longitudinally to fill the projection; this would come into play in our analysis. The images (fig. 5) showed Triton from +66.79° to -67.07° latitude and +180° to -180° longitude. When loaded into our image processing software, each mosaic was 512 x 260 pixels. Each pixel represented an individual data value. Note that not all the areas were filled due to the limited number of high resolution images from Voyager II. The mosaic making process created a few seams that could still been seen and were taken into account when analyzing the data.

The mosaics were created by Joel Mosher, a former Voyager imaging team member. The pixel values range from 0 to 441 for the clear mosaic, 0 to 213 for the UV, and 0 to 11333 for the green. Though the units for the pixel values were not readily known, Mosher assured us that the values were linearly proportional to albedo. Our comparison contrasted relative intensities rather than actual values, so the exact units were not necessary

The imaging processing software we used was IDL (Interactive Data Language), written by Research Systems, Inc. It is a very flexible system that allows for easy manipulation and display of large data sets, particularly images. An image takes the form of a

matrix having dimensions that match the image's pixel dimensions. Such a matrix can be operated on by standard mathematical functions, or by helpful preprogrammed procedures. For repetitive or complicated tasks that aren't covered in the standard library, user written procedures are relatively easy to create in IDL.

Our primary interest was the comparison of the clear mosaic with the UV. The green mosaic was helpful as a rough comparison, but was not used in our actual data processing. Although a comparison between the green filter and the UV filter would be a cleaner comparison (see fig. 4), we decided that the stronger signal from the clear mosaic would offset the slight overlap. We tried two different methods of comparison. The goal was to find areas where the clear mosaic was bright and the UV was dark, indicating UV absorbing material.

A direct ratio between the clear mosaic and the UV mosaic was an attractive option. However, we were concerned that it might produce more areas of correlation than there really are. If, for example, we took the clear mosaic and divided it by the UV, areas where the UV is near average while the clear is unusually bright would appear the same to us as areas we are looking for: bright in the clear and dark in the UV. We needed to find a way of taking a ratio that would eliminate these false results.

Our first method started with the creation of "contrast" images from the mosaics. An average pixel value was taken from the clear and UV mosaics. The averages were taken across the width of the image from row 161 up to the top (row 161 is the first complete row

of pixels). These new "contrast" mosaics were made according to the following equation:

$$\text{"contrast" mosaic} = \frac{(\text{mosaic} - \text{mosaic average})}{\text{mosaic average}}$$

These "contrast" mosaics were consequently centered on zero. We could then use these new mosaics to compare directly the original mosaics.

We took a modified ratio between these clear and UV "contrast" mosaics. We divided the difference of the clear contrast mosaic and the UV contrast mosaic by the absolute value of their sum. More clearly:

$$\text{comparison} = \frac{(\text{clear contrast} - \text{UV contrast})}{|\text{clear contrast} + \text{UV contrast}|}$$

Fig. 6 shows the comparison image that resulted from our analysis. This method avoided the problem of the direct ratio mentioned earlier. Since the images were centered on zero, the denominator would be near zero for areas in which we were interested. For the same areas the numerator would be quite large. This resulted in a comparison image where bright pixels indicated areas that were bright in the clear and dark in the UV.

Although this result was very interesting we needed a more clear-cut method of finding the correlation for which we were looking. Another problem of the first method was that the average we took was biased towards the polar regions. As noted earlier,

these were Mercator projections; the areas of higher latitudes were stretched. These areas naturally took up a disproportional number of image pixels and influenced the average.

We tried a second method that compared directly the standard deviations of each mosaic. We looked for places where the clear mosaic was one standard deviation higher than average and the UV mosaic was one standard deviation lower than average. However, before this could be accomplished we needed to develop a way of taking image averages and standard deviations corrected for the Mercator projection bias.

In calculating a weighted image average we followed the procedure of dividing the weighted sum by the sum of the weights:

$$\text{weighted average} = \frac{\sum x_i w_i}{\sum w_i}$$

where w_i is the weighting function; in our case the cosine of the latitude. We totaled the pixel values for each row and multiplied it by the cosine of that row's latitude on the moon. This was then summed over all the rows and divided by the sum of the cosines for each row.

Using this method we calculated the image averages for both clear and UV mosaics. The mosaics were divided by these new averages to obtain normalized mosaics. When normalized we could compare these images directly, making the unknown pixel units irrelevant. The weighted average procedure was performed again on

the normalized images with a resulting mean of one, confirming that our procedure was correct.

After some thought we chose a suitable method for calculating a weighted standard deviation. In IDL there is a procedure called CONGRID that can resize a row's number of pixels evenly, either expanding it or contracting it while keeping the data intrinsically the same. When contracting a row the data will be altered slightly, but the overall pattern will be preserved in the fewer pixels. CONGRID was used to resize the rows in both mosaics according to a cosine function of latitude. STDEV, a pre-programmed IDL function, was then used to find the standard deviation of these resized mosaics. With fewer polar pixels as compared to equatorial pixels, these standard deviations were automatically corrected for the Mercator projection.

With the correct averages and standard deviations known we then performed a more clear-cut comparison of our two mosaics. We looked first at places were the clear mosaic was at least one standard deviation higher than the average. A new image reflecting this was made. All the pixels of the clear mosaic one standard deviation or more then the mean were given a value of one, all other pixels were set to zero (fig. 7). Similarly, we looked at places one standard deviation or more lower than the mean on the UV mosaic. Pixels that fit our stipulation were assigned a one and all others set to zero (fig. 8).

A final comparison consisted of multiplying the two new images together, resulting in a comparison image. Only pixels that were valued one on *both* former images were valued one on the

comparison image (fig. 9a). We then saw areas where the clear and UV mosaics were correlated, indicating UV absorption. A second comparison was done employing the same method again at a two sigma or more variation from the mean (fig. 9b).

III. Results and Further Work

Our first method as described above was to compare the difference of the images divided by the absolute value of the sum of the images. This resulted in a comparison map (fig. 6) From the method used, pixels on this map are places demonstrating UV absorption. There were a few spotty areas in the equatorial region near 0° longitude (center of the image) that responded to our analysis. Yet overall, this map shows no distinct areas of UV absorption.

The second method involved finding pixels in the clear mosaic that were a multiple of standard deviation higher than the mean while being a multiple of standard deviation lower than the mean in the UV mosaic. We tried two cases: one and two standard deviations higher and lower, respectively. The one standard deviation result (fig. 9a) also showed spotty UV absorbing in the equatorial region near 0° longitude as well as another small equatorial region near +150° longitude. The two standard deviation case had a handful of pixels in the equatorial region near 0° longitude also (fig. 9b).

The few small areas that appeared in our second method were promising. The one standard deviation case shows this most clearly.

However, the laboratory spectra of the most probable UV absorbing material (fig. 3c) suggests that at least two standard deviations of inverse correlation were needed to clearly identify them. The two standard deviation comparison showed too few pixels to be significant. We concluded there was *no* clear large scale inverse correlation between the clear mosaic and the UV mosaic. This meant there was no definite areas of UV absorbers on Triton in the areas covered by the mosaics.

Further studies in two areas can advance this initial analysis. Firstly, using raw Voyager II images, with resolutions better than those of the mosaics we can study small scale distribution of UV absorbers. The mosaics were created so that all of the surface was represented at one continuous resolution, although not the best possible resolution. Voyager II took a few images at much higher resolutions, both in the clear and UV range. Using the same methods of comparison that were used on the mosaics, we hope to analyze smaller detail areas for UV absorbers.

Secondly, we can further classify these UV absorbing materials by carefully studying the UV spectra of Triton. Voyager II's UV filter transmittance (fig. 4) is limited in its view of the UV. Using the IUE (International Ultraviolet Explorer) and the Hubble space telescope, continuous spectra can be taken, going further into the UV than Voyager II. Comparing these spectra with laboratory spectra, we hope to further restrict what these UV absorbing materials might be.

This was a part of an NDAP (Neptune Data Analysis Project) on which Dr. Stern is currently working. Mapping the large scale spatial

distribution of UV absorbing material was a small constituent of an extended project. The goal of this project is to typify Triton's geological structure. The two other steps mentioned are already under way at Southwest Research Institute as well as JPL. When completed, it's expected our project will provide more information not only on Triton, but on the species of outer solar system bodies of which it is a member.

References

Benesh M. & Jepsen P.; "Voyager Imaging Science Subsystem Calibration Report"; Jet Propulsion Laboratory, internal document 618-802; July 31, 1978

Croft S. K., Kargel J. S., Kirk R. L., Moore J. M., Schenk P. M., & Strom R. G.; "The Geology of Triton"; awaiting publication in *University of Arizona Press*; submitted March 4, 1993

Hillier J., Veverka J., & Helfenstein P., & McEwen A.; "The Wavelength Dependance of Triton's Light Curve"; *Journal of Geophysical Research*, vol.96, supplement; pages 19,211-19,215

McEwen S.; "Global Color and Albedo Variations on Triton"; *Geophysical Research Letters* vol.17 no.10; pages 1,765-1,768; September, 1990

Stern A.; "*A Proposal for* the Distribution and Nature of UV Absorbers on Triton's Surface"; Southwest Research Internal document; Proposal No. 15-13170; submitted to NASA June 1992

Yoemans, D.; *Comets: A Chronological History of Observation, Science, Myth, and Folklore*; John Wiley & Sons, Inc.; New York, 1991

Captions to Figures

fig.1a - Ground-based spectrum of Triton taken at McDonald Observatory. Notice the red slope starting around 490 nm indicating UV absorption.

fig. 1b - A spectral continuation of fig. 1a taken with the Hubble Space Telescope. Again notice the steadily decreasing albedo in the UV.

fig. 1c - McEwen (1990) divided Triton into 6 different geological regions. This graph shows the mean spectral reflectivities of each one of these regions. Notice that all but one demonstrate UV absorption.

fig. 2a - A lightcurve amplitude graph of Triton, delineated into the six different filters used aboard Voyager II. The UV amplitude is greater than the other filters.

fig. 2b - A lightcurve amplitude graph made from ground-based observations, Voyager II, and International Ultraviolet Observer data. Again note the high UV lightcurve amplitude as compare with visual wavelengths.

fig. 3a - Laboratory spectra of known Triton surface materials and possible UV absorbers. Note how the SO_2 drops off in the UV before the known surface materials.

fig. 3b - Spectra of possible UV absorbers on Triton. Again not the UV drop off in reflectance.

fig. 3c - Spectrum of most probable Triton UV absorber: SO_2 .

fig. 4 - Tranmittances of Voyager II's clear, green and UV filters.

fig. 5a - The UV mosaic we used in our analysis.

fig. 5b - The clear mosaic.

fig. 6 - The comparison mosaic created from out first analysis method. Note the bright area just slightly left of the center of the image, representing an area of correlation.

fig. 7a - The clear mosaic showing areas that are at least one standard deviation above the mean.

fig. 7b - The clear mosaic showing areas that are at least two standard deviations above the mean.

fig. 8a - The UV mosaic showing areas that are at least one standard deviation lower than the mean.

fig. 8b - The UV mosaic showing areas that are at least two standard deviations lower than the mean.

fig. 9a - The resulting mosaic created by multiplying fig. 7a and 8a together. This shows pixels that are at least one standard deviation ABOVE the mean on the CLEAR mosaic AND at least one standard deviation BELOW the mean on the UV mosaic.

fig. 9b - The resulting mosaic created by multiplying fig. 7b and 8b together. This shows pixels that are at least two standard deviations ABOVE the mean on the CLEAR mosaic AND at least two standard deviations BELOW the mean on the UV mosaic.

fig. 10a - The clear mosaic depicted in a 3D surface plot.

fig. 10b - The UV mosaic depicted in a 3D surface plot.

table 1 - Specifications of Voyager II's camera filters.

table 2 - List of Voyager II images used in creating the mosaics. They are listed together with their time to closest approach, image catalog number, and filter.

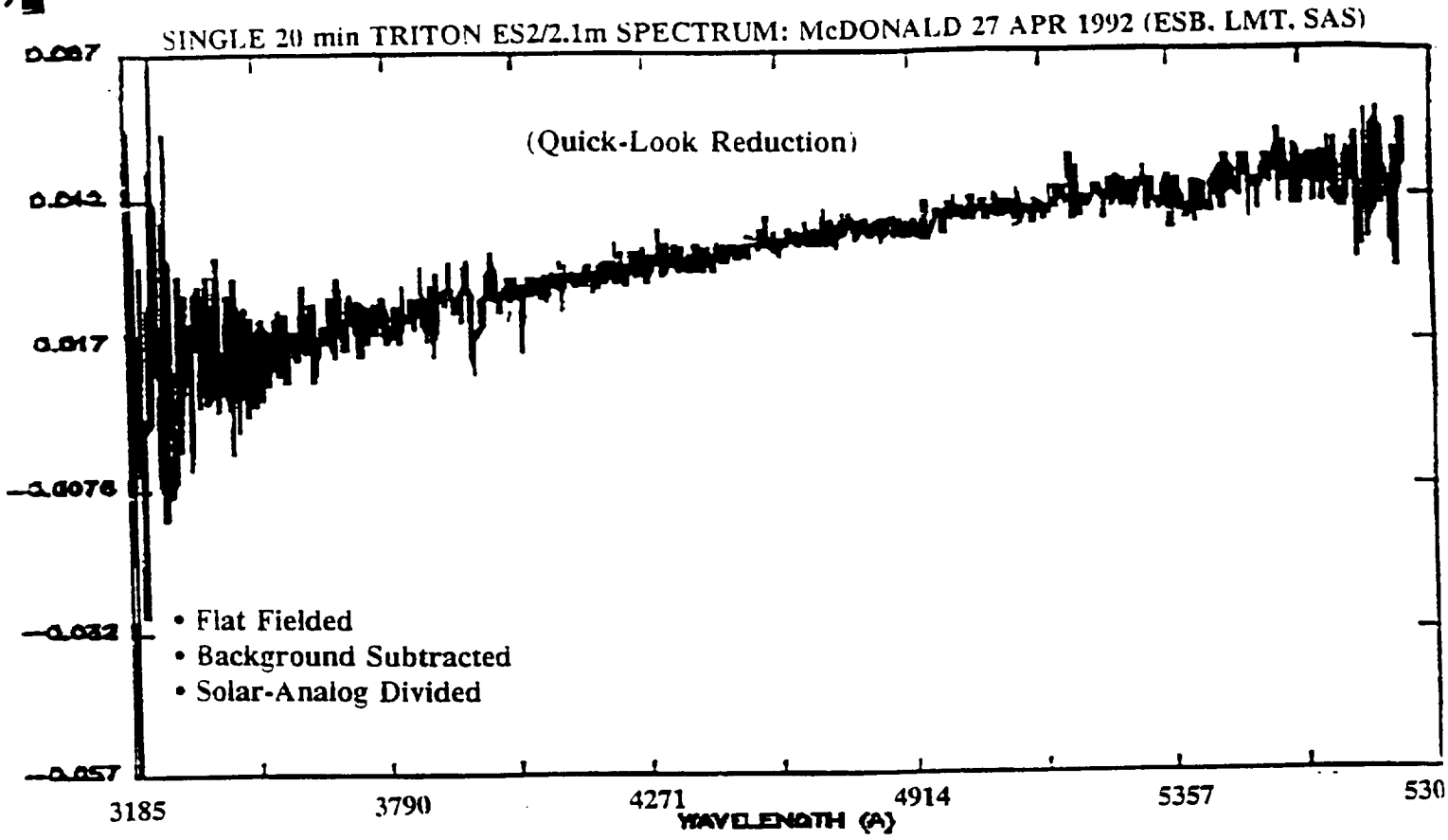

fig.1a

ORIGINAL PAGE IS
OF POOR QUALITY

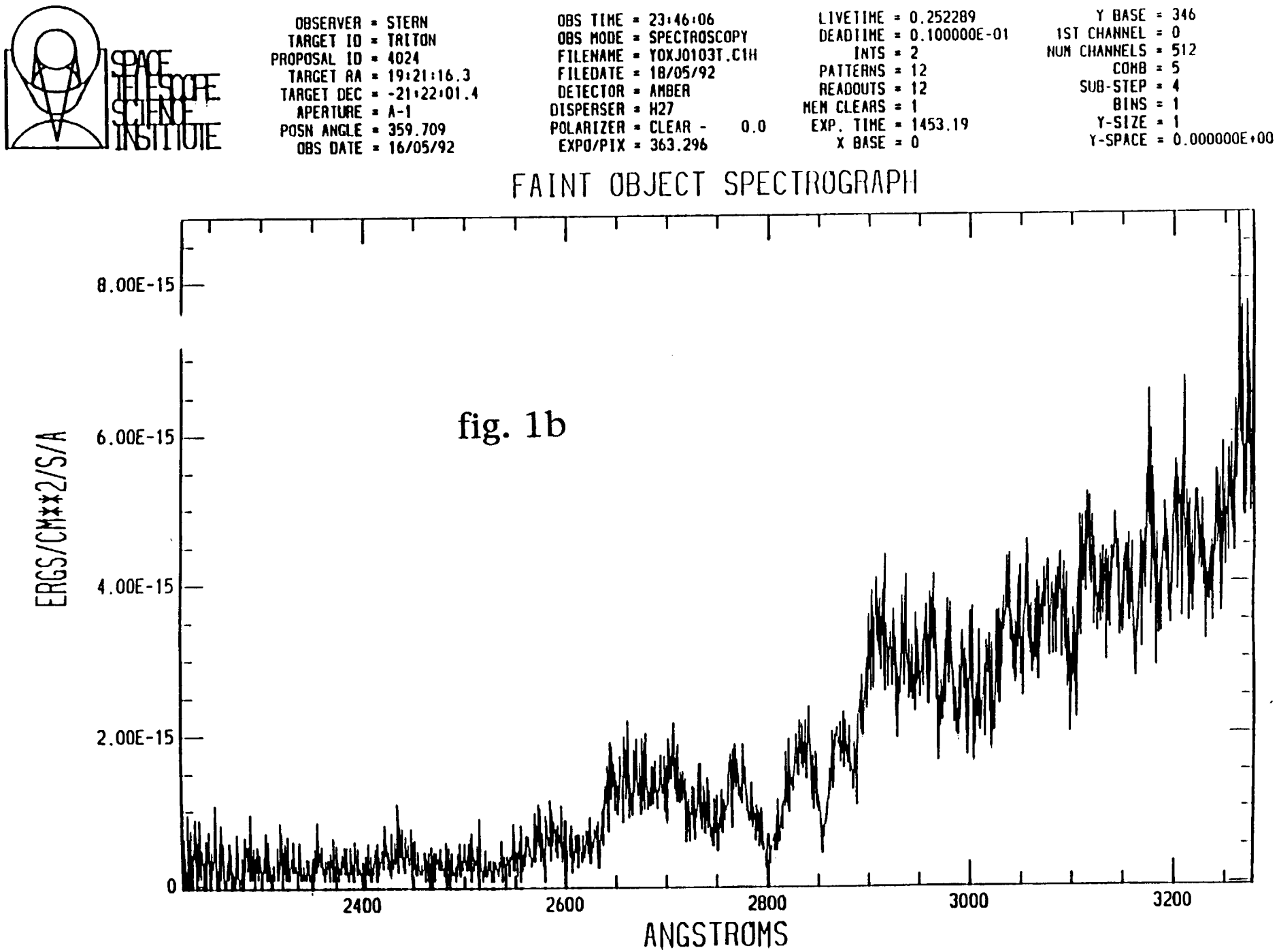

ORIGINAL PAGE IS OF POOR QUALITY

Fig. 1b

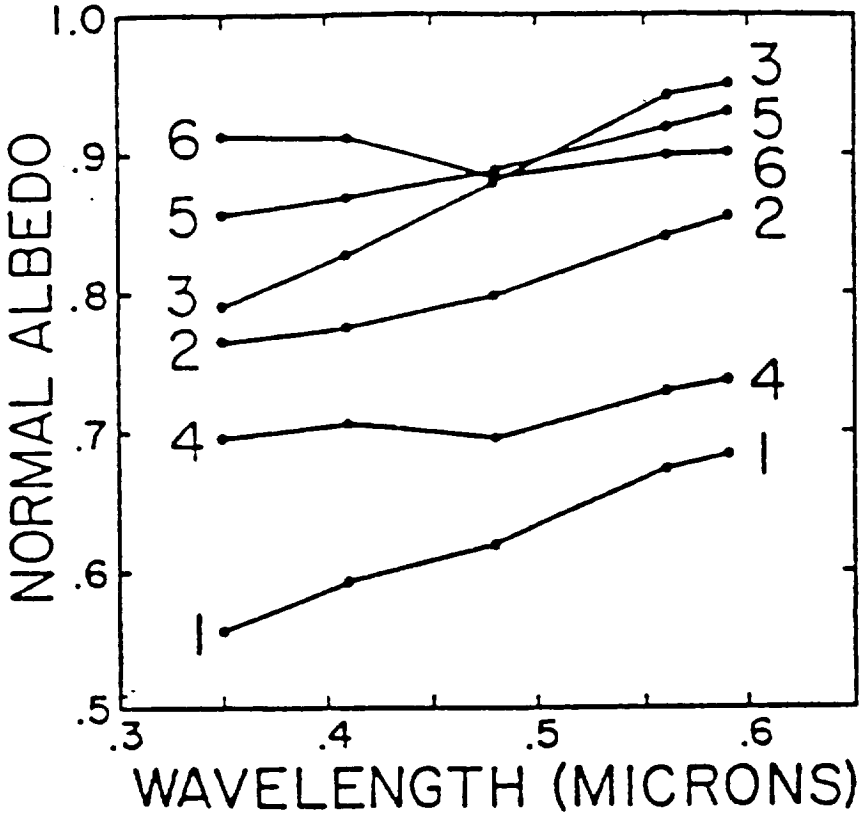

Mean spectral reflectivities (in the five Voyager color filters) of the six spectral units.

fig. 1c

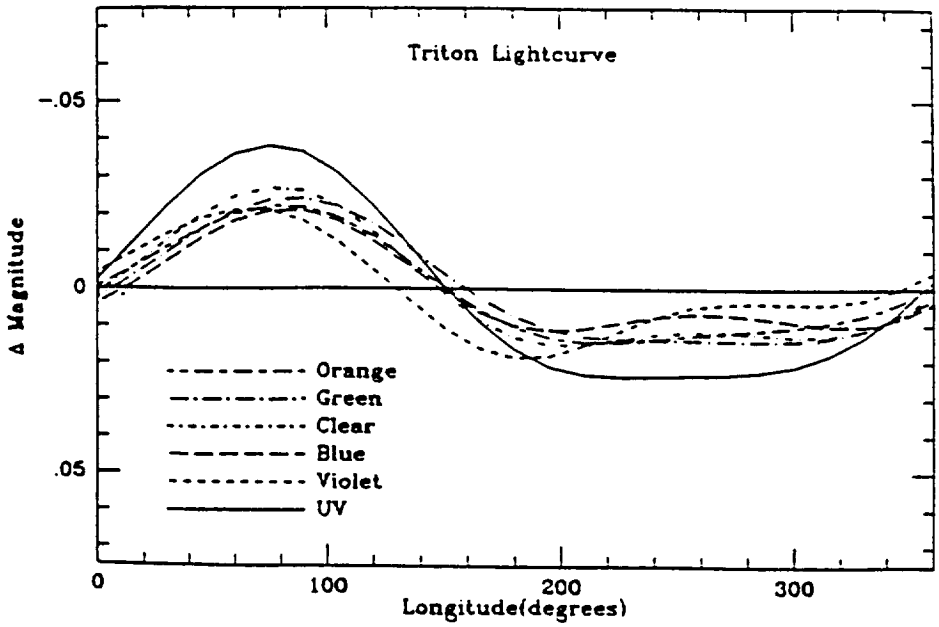

Fig. 2. Wavelength dependence of Triton's light curve over the Voyager filter wavelengths. Shown are the light curves predicted from the Voyager normal albedo maps (see text) through all of the Voyager narrow-angle camera filters.

fig. 2a

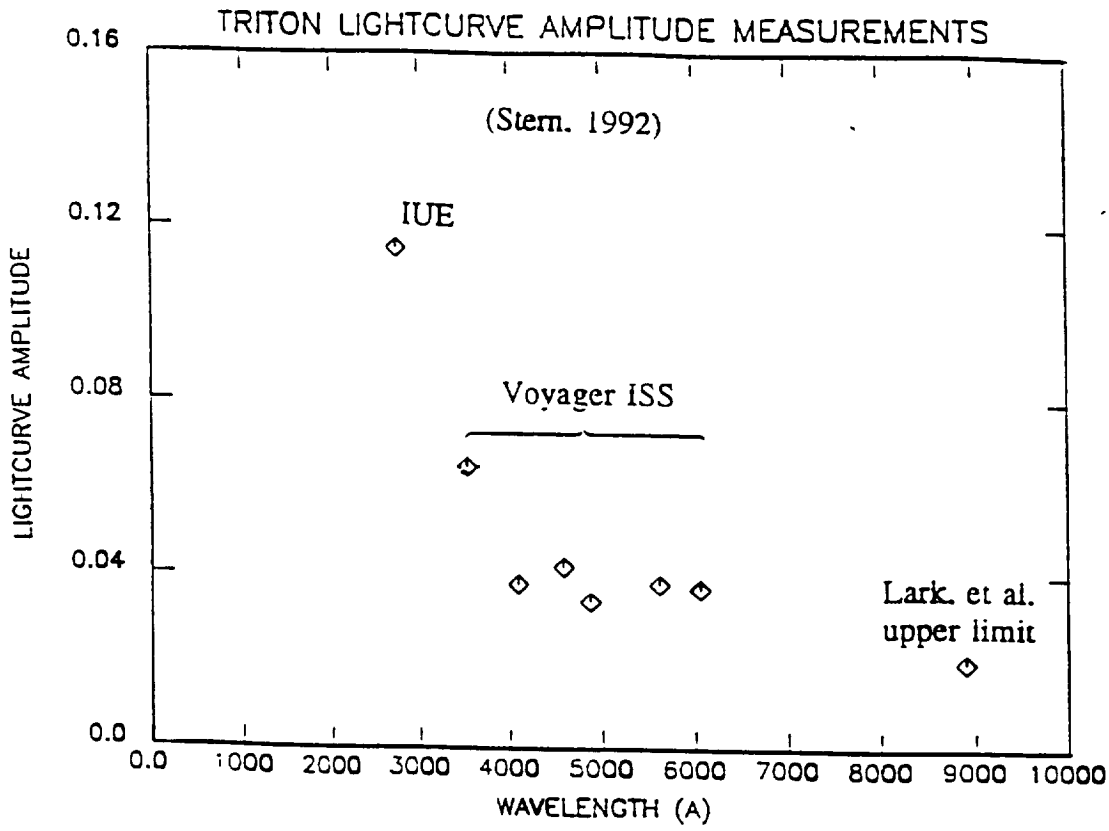
TRITON LIGHTCURVE AMPLITUDE MEASUREMENTS
(Stern. 1992)
IUE
Voyager ISS
Lark. et al.
upper limit
LIGHTCURVE AMPLITUDE
0.16
0.12
0.08
0.04
0.0
0.0
1000
2000
3000
4000
5000
6000
7000
8000
9000
10000
WAVELENGTH (A)

fig. 2b

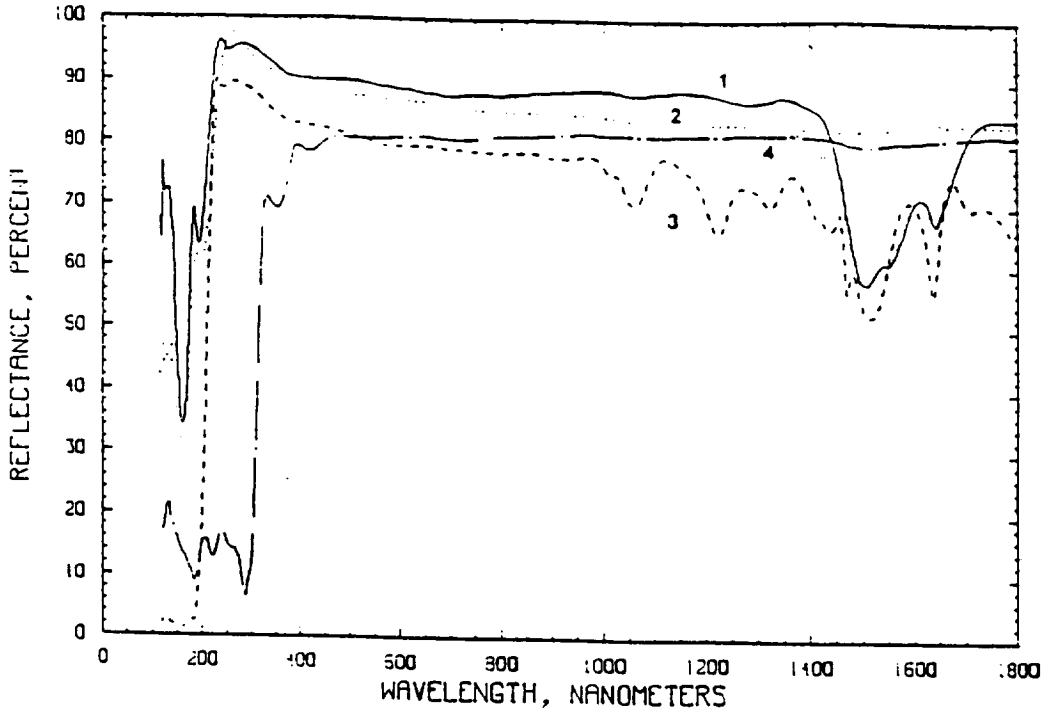

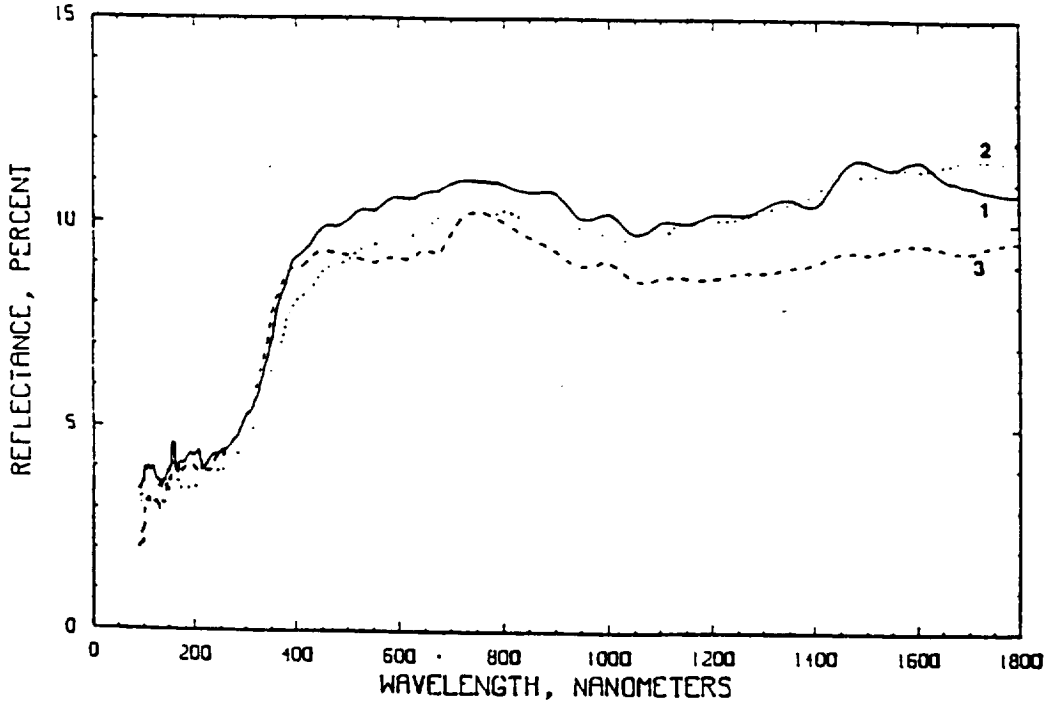

Reflectance spectra of frosts of gases as a function of wavelength in nanometers from Wagner. Hapke.and Wells 1987. Curve 1 is for H_2O. 2 for CO_2. 3 for NH_3. and 4 for SO_2. Copyright Academic Press. By permission.

Same as above but for powdered samples of carbonaceous chrondrites. Curve 1 is for Warrenton (CO_3). 2 for Allende (CV_3) and 3 for Karoonda (CO_3). Copyright Academic Press. By permission.

fig. 3a

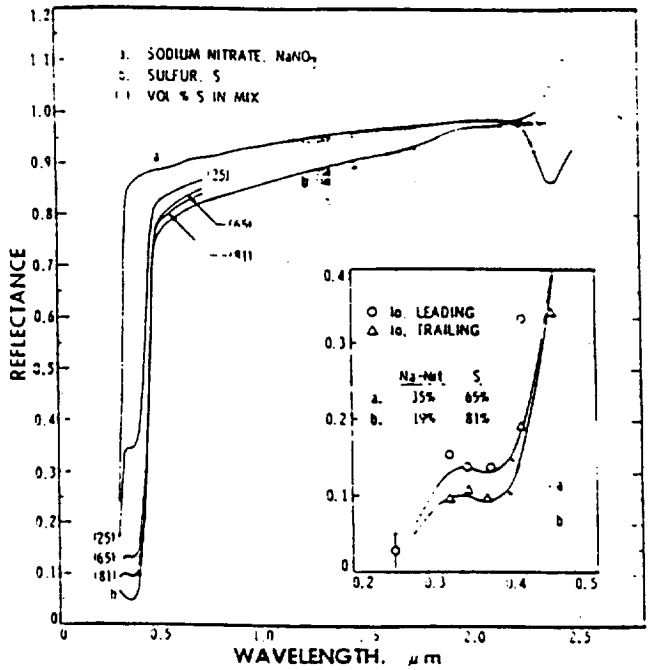

Spectra of sodium nitrate, sulfur, and mixtures. Inset shows detailed comparison of spectra of sodium nitrate/sulfur mixtures with Io data from the ultraviolet.

fig. 3b

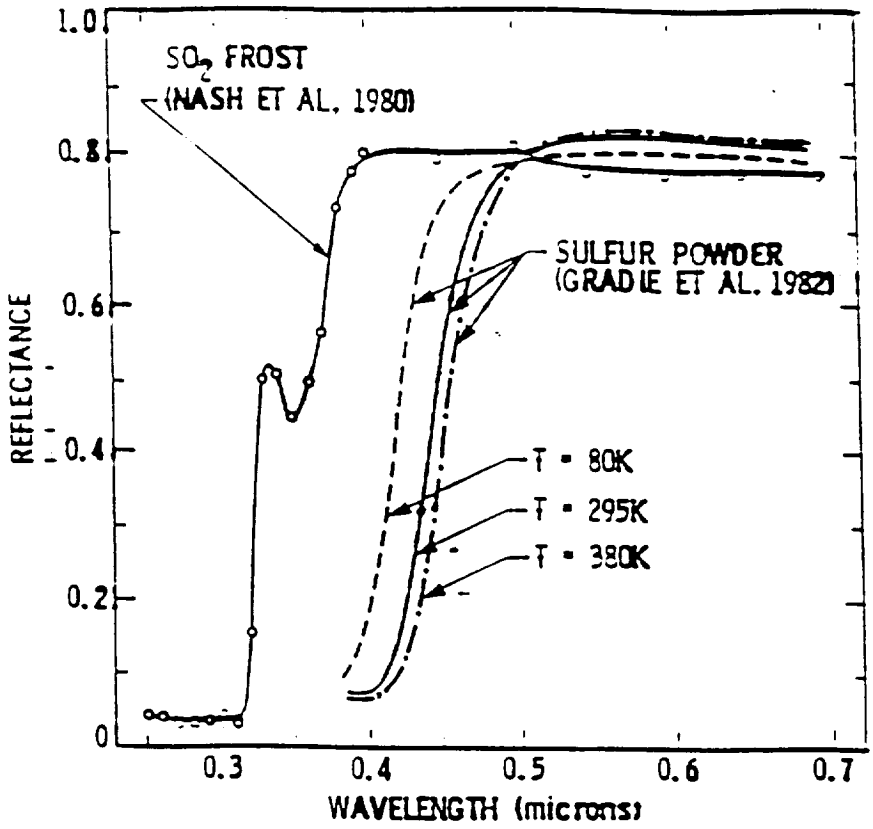

Laboratory reflectance spectra of sulfur powder and sulfur dioxide frost. Both materials have a steep absorption band edge in the ultraviolet and are otherwise bright and featureless in the visible and near infrared. The absorption edge position of sulfur is temperature sensitive, shifting to shorter wavelength as temperature decreases; at typical Io surface temperature (135 K) ordinary yellow sulfur appears white. In the ultraviolet near 0.25 to 0.30 μm, SO_2 frost is less reflective than sulfur by ~1/2. (Nash, et al 1986)

fig. 3c

ORIGINAL PAGE IS
OF POOR QUALITY

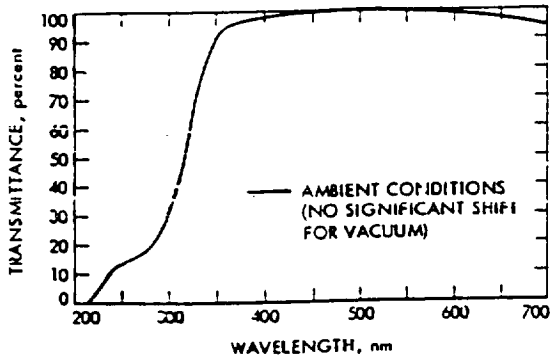

Spectral transmittance, clear filter 4BN and 9BW (position narrow-angle 0, 4 and wide-angle 2)

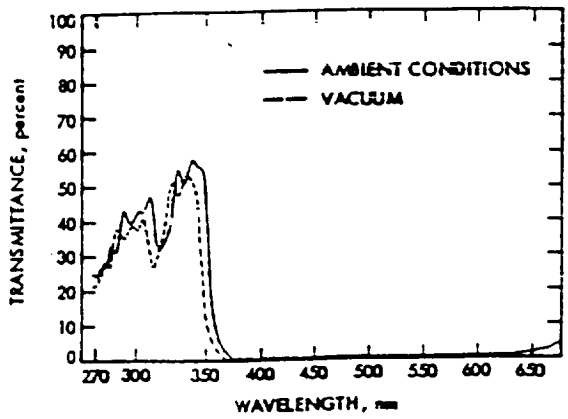

Spectral transmittance, ultraviolet filter 1 AN (position narrow-angle 7)

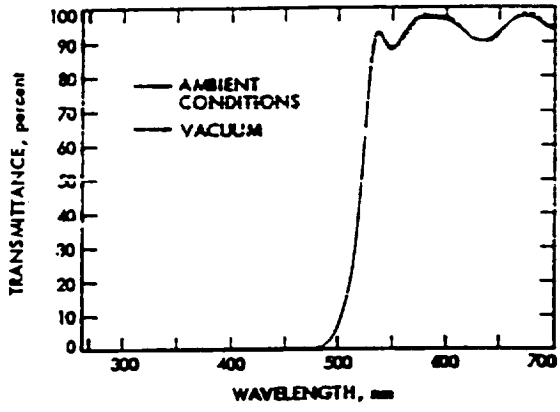

Spectral transmittance, green filter 3BN (position narrow-angle 5 and 6)

fig. 4

fig. 5a

ORIGINAL PAGE IS
OF POOR QUALITY

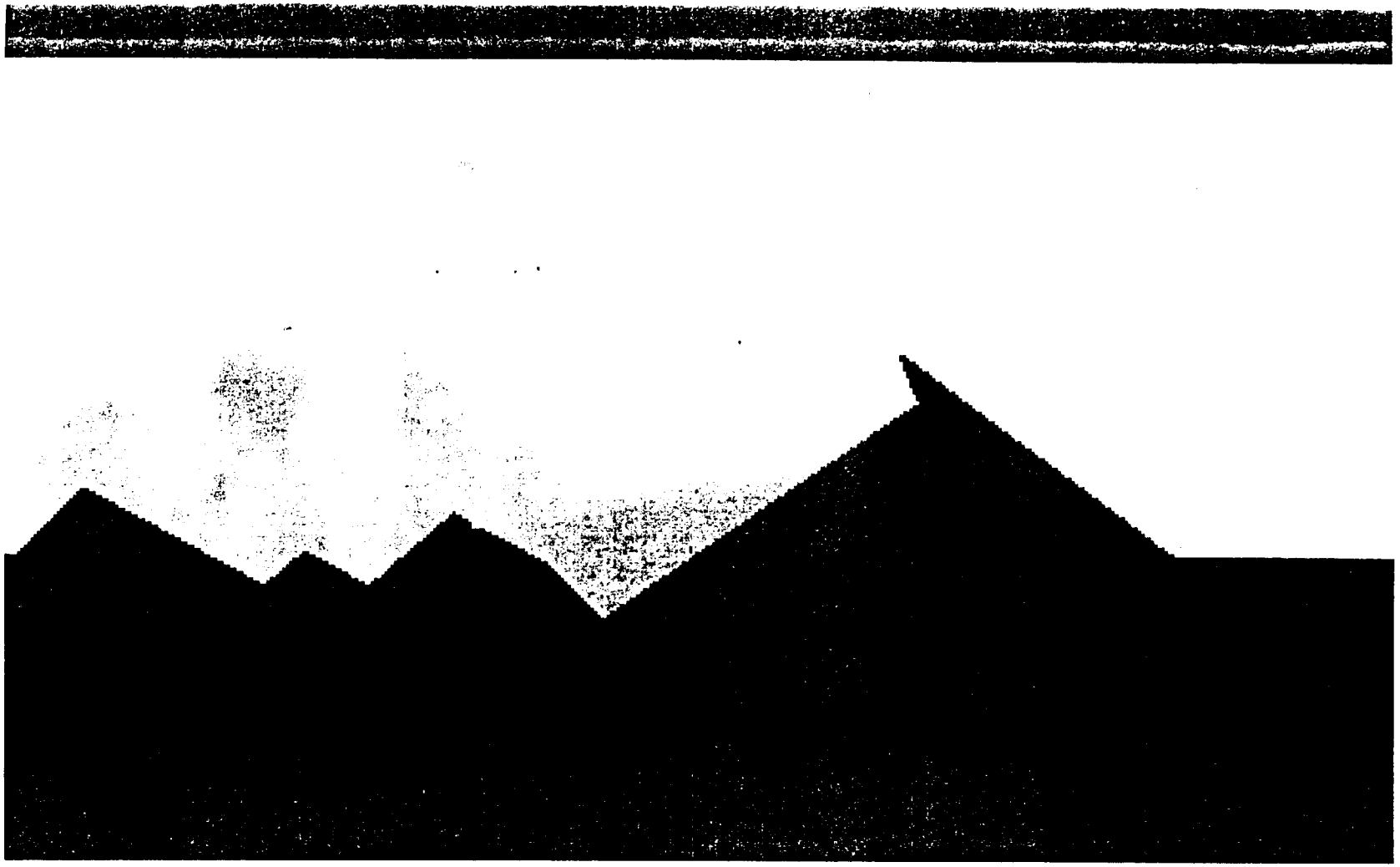

fig. 5b

ORIGINAL PAGE IS
OF POOR QUALITY

fig. 6

ORIGINAL PAGE IS
OF POOR QUALITY

fig. 7a

ORIGINAL PAGE IS
OF POOR QUALITY

ORIGINAL PAGE IS
OF POOR QUALITY

fig. 7b

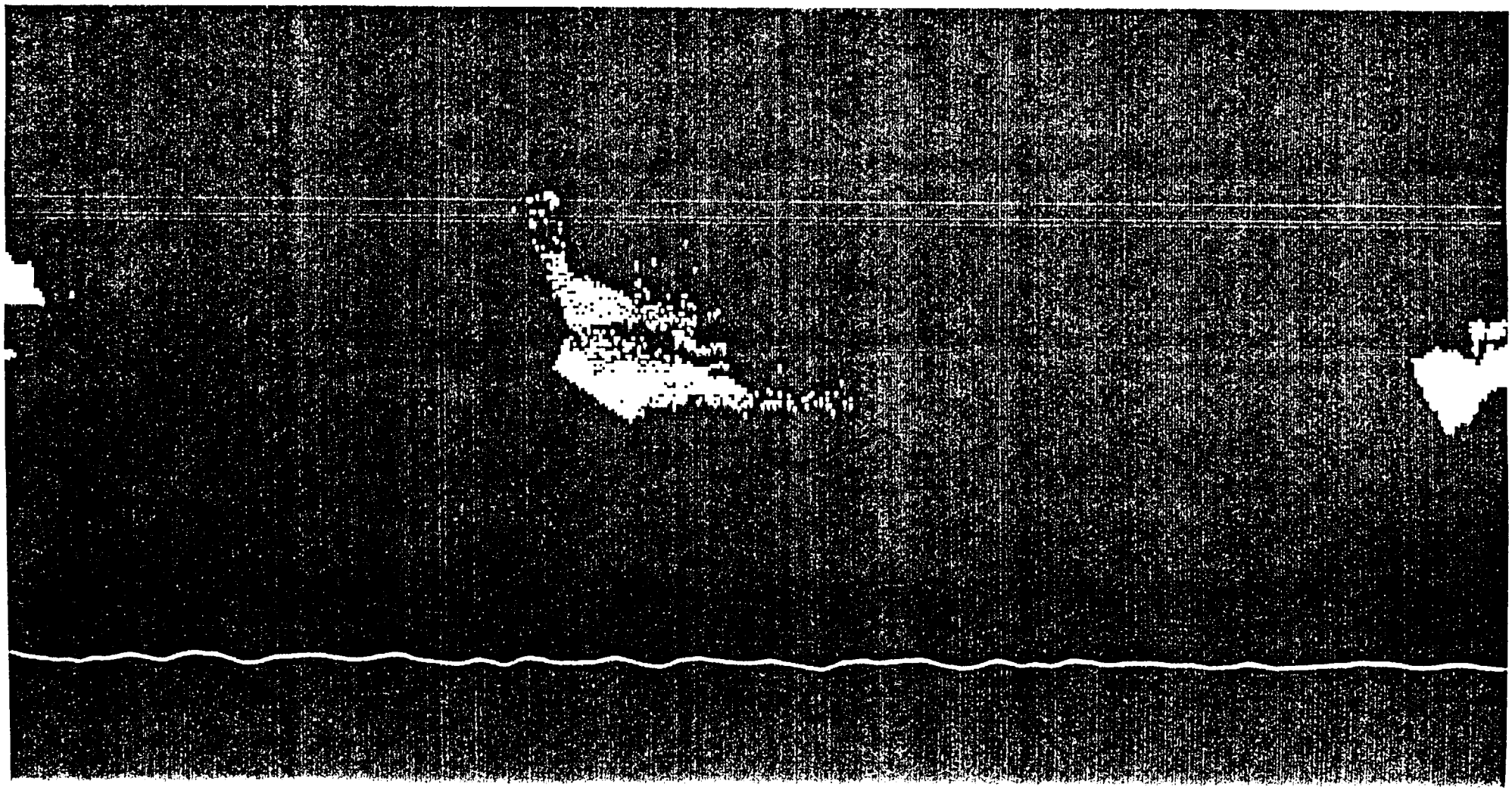

fig. 8a

ORIGINAL PAGE IS
OF POOR QUALITY

fig. 8b

ORIGINAL PAGE IS
OF POOR QUALITY

fig. 9a

ORIGINAL PAGE IS
OF POOR QUALITY

fig. 9b

ORIGINAL PAGE IS
OF POOR QUALITY

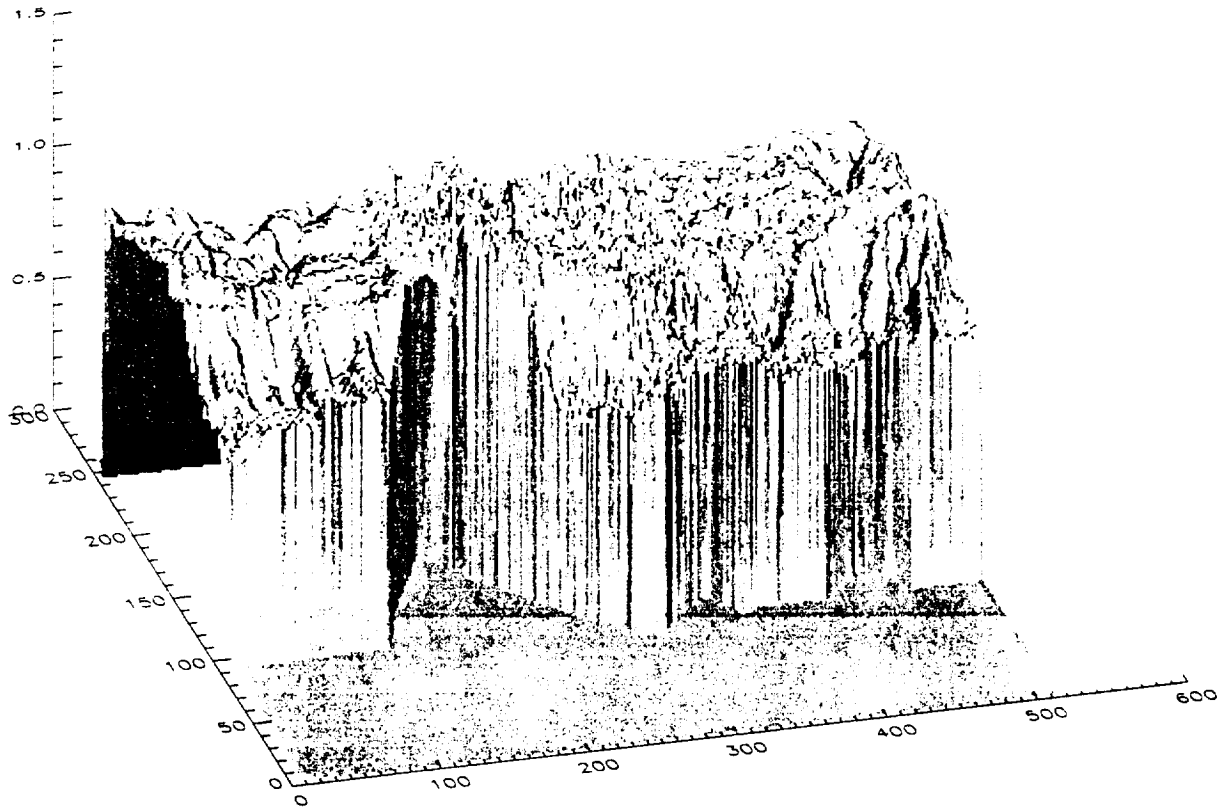

fig. 10a

ORIGINAL PAGE IS
OF POOR QUALITY

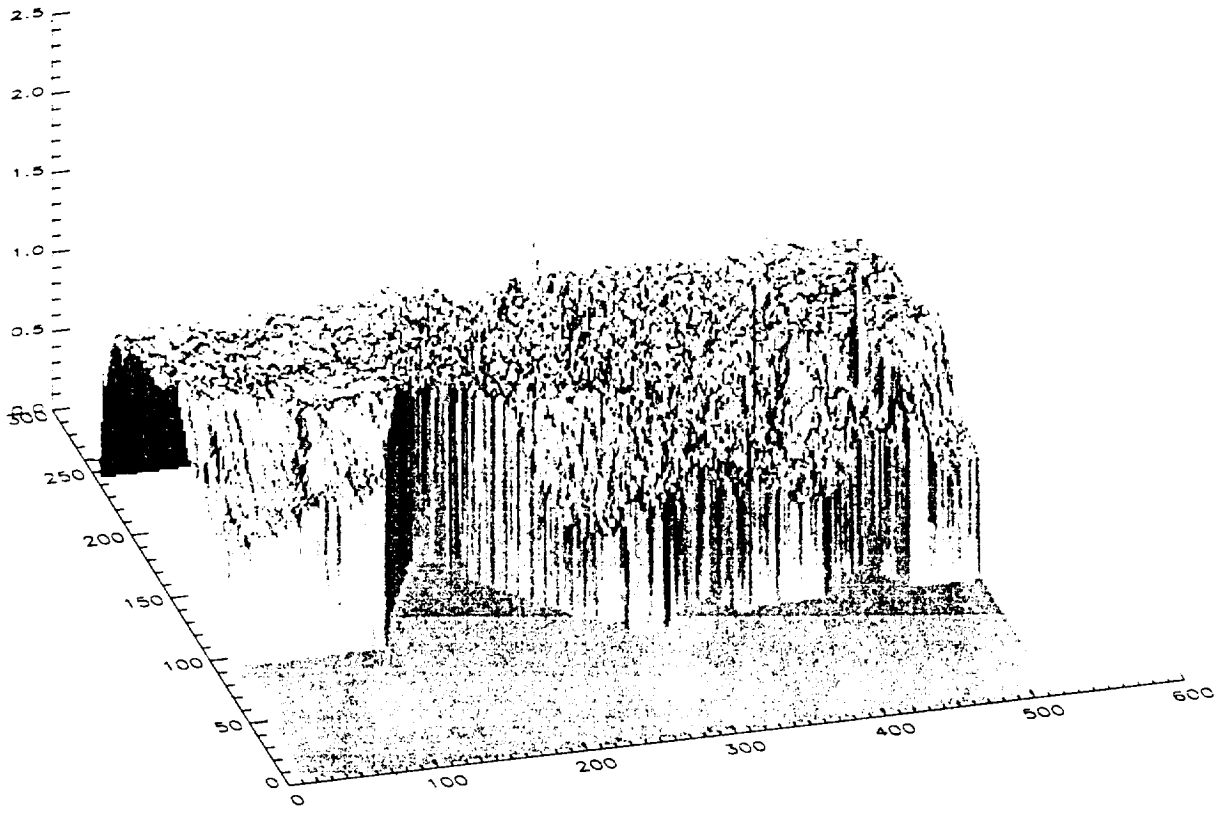

fig. 10b

ORIGINAL PAGE IS
OF POOR QUALITY

Table A typical set of ISS camera filters

ISS camera	Filter-wheel position	Filter	Filter class ID	Wavelength, Å	Type
Narrow-angle	0	Clear	4BN	—	Interference
	1	Violet	2AN	4000 ±500	
	2	Blue	3AN	4800 ±500	
	3	Orange	7BW (thick)	>5700	
	4	Clear	4BN	—	
	5	Green	3BN	>5300	
	6	Green	3BN	>5300	
	7	UV	1AN	3250 ±450	
Wide-angle	0	Methane (6190)	2CW	6190 ±50	
	1	Blue	6AW	4800 ±500	
	2	Clear	9BW	—	
	3	Violet	4AW	4000 ±500	
	4	Sodium-D	1CW	5890	
	5	Green	6BW	>5300	
	6	Methane (Uranus)	3CW	5410 ±50	
	7	Orange	8BW	>5900	

table 1

Clear filtered images used:
1127755
1129147
1129855
1130545
1131314
1133837
1134834
1137148
1137709
1138709
1139303
1139330
1139340

Green filtered images used:
1131336
1129913
1129205
1127807
1126628
1133859
1134856
1137221
1137721
1138703
1139311
1139317

UV filtered images used:
1126642
1127814
1129212
1129920
1131400
1133923
1134920
1138715
1139313
1139319
1137727
1137245

table 2

Appendix 2

THE SPATIAL DISTRIBUTION OF UV-ABSORBING REGIONS ON TRITON

Flynn B., Stern A., Buratti B., Schenk P., and Trafton L.

Substantial evidence suggests that a UV Spectrally Absorbing Material (UV-SAM) exists on Triton's surface. This evidence is found in the positive slope in Triton's spectrum from the UV to the near-IR, and the increasing contrast in Triton's light curve in the blue and UV. Although it is now widely thought that UV-SAMs exist on Triton, little is known about their distribution and spectral properties.

We present the first results of an ongoing study using Voyager 2 images, IUE and HST spectra, and a geological map of Triton to determine the spatial distribution and geological context of the UV-SAMs on Triton. The goal of this project is to determine if UV-SAMs on Triton are correlated with geologic wind streaks, craters, calderas, geomorphic/topographic units, regions containing (or lacking) volatile frosts, or some other process (e.g., magnetospheric interactions). The study of the Voyager imaging data is taking place in two phases: (1) Search for large-scale (10s-100s of km) UV-absorbing regions using global, medium-resolution maps of Triton; and (2) a study of high-resolution UV-visible image pairs to look for UV-SAM regions on a small spatial scale ($\sim$10 km).

As a result of Phase 1 of our study, we find a distinct UV-dark region $\simeq$700$\times$1900 km in size and centered near $+20°$ longitude and $-25°$ latitude. The region correlates well with a geological unit containing maculae (spotted terrain) and wind streaks. The UV-absorbing region abuts a high-albedo region, lying just to north, that may be composed of relatively uncontaminated, clean ices. The positioning of the UV-dark region and the clean-ice region suggests a possible dynamic relationship involving volatile transport between the two units.